J Appl Electrochem (2008) 38:1011–1018
DOI 10.1007/s10800-008-9527-1

ORIGINAL PAPER

Simulation of mass transport in SOFC composite electrodes

Marco Cannarozzo · Adriana Del Borghi · Paola Costamagna

Received: 8 October 2007 / Revised: 14 February 2008 / Accepted: 19 February 2008 / Published online: 11 March 2008

Abstract The anodes used in SOFCs are composites, formed by a mixture of nickel and YSZ particles. This paper presents a model for this type of electrode, taking mass transport effects into account. The effect of the operating conditions, such as temperature and pressure, is discussed. Also, the effect of the choice of the geometrical parameters, such as electrode thickness and particle radius, on the electrode performance is analysed in detail. In particular, the electrode losses display a minimum for a well-defined radius of the electrode particles, which is related to a trade-off between activation and concentration losses.

Keywords Solid oxide fuel cell · Composite electrodes · Cermets · Microstructure

Nomenclature

A	Active area per unit volume ($cm^2\ cm^{-3}$)
D	Diffusivity ($cm^2\ s^{-1}$)
F	Faraday's constant (96,487 C mol^{-1})
I	Overall electrode current density (A cm^{-2})
i	Current density in the electrode (A cm^{-2})
i_0	Exchange current density (A cm^{-2})
i_n	Transfer current density per unit of active area (A cm^{-2})
N	Molar flux of the component i (mol $cm^{-2}\ s^{-1}$)
p_i	Partial pressure of i component (atm)
p_{ref}	Reference pressure (atm)
P	Particle dimension ratio (r_{io}/r_{el})
r	Particle radius (cm)
R	Universal gas constant (J $mol^{-1}\ K^{-1}$)
r_{pore}	Mean pore radius (cm)
t	Overall electrode thickness (cm)
T	Temperature (K)
V	Electric potential (V)
x	Main co-ordinate (cm)
x_i	Molar fraction (of i component) (−)

Greek symbols

β	Transfer coefficient
γ	Pre-exponential factor (Eq. 8)
ε	Porosity
η	Overpotential (V)
ρ	Resistivity (ohm m)
σ	Collision diameter (A)
τ	Tortuosity
φ	Volumetric fraction of electronic conductor
Ω	Collision integral

Subscript

el	Electronic conductor
io	Ionic conductor
K	Knudsen

Superscript

0	inlet
eff	effective

1 Introduction

Among the different types of fuel cells, solid oxide fuel cells (SOFCs) [1, 2] are receiving worldwide attention due to a number of interesting features. For example, due to their high operating temperature (about 900–1,000 °C), they are suitable for coupling with a microturbine in a

M. Cannarozzo · A. D. Borghi · P. Costamagna (✉)
DICHEP, University of Genoa, Via Opera Pia 15,
16145 Genoa, Italy
e-mail: paola.costamagna@unige.it

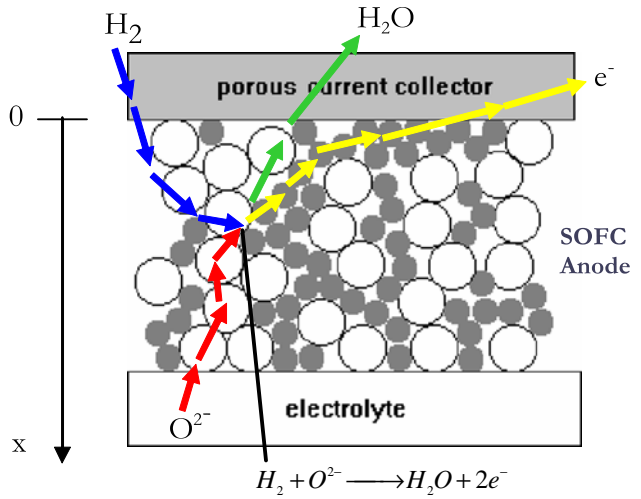

Fig. 1 Composite SOFC anode

hybrid system, with an overall system efficiency which is predicted to reach values as high as 65–70% [2]. Other advantages of SOFCs are the possibility of employing a variety of fuels, and the limited need for precious materials. The electrolyte is a ceramic (usually Y_2O_3 stabilized ZrO_2 (YSZ)); the presence of the solid electrolyte allows the manufacturing of various geometries, such as planar, tubular and integrated planar (IP-SOFC), which have different features in terms of manufacturing costs, thermal expansion resistance and electrochemical performance.

Composite electrodes (Fig. 1) are now the state-of-the-art for SOFC applications [2–5]. Composite electrodes consist of a mixture of ionic and electronic conducting particles. At present, the most used materials for this application are a cermet (Ni + YSZ) for the anode and a composite (LSM + YSZ) for the cathode, where LSM is $La_{0.85}Sr_{0.16}MnO_3$, an electron conducting perovskite material [2]. Composite electrodes have several advantages over non-composite ones. The first benefit consists of the reduction of thermal stress effects; as a matter of fact, the thermal expansion coefficient of a composite anode made of Ni + YSZ is about 12.5×10^{-6} K^{-1}, a value closer to the electrolyte expansion coefficient (13.3×10^{-6} K^{-1}) than that of a pure nickel electrode (11×10^{-6} K^{-1}) [2]. This also allows better adhesion of the different layers at the operating temperature. This is important, as the effect of strain caused by the differential thermal expansion is a common problem for SOFCs. A further, and maybe the most important, advantage of using composite electrodes is the extension of the triple-phase boundary (TPB) throughout the electrode. The TPB is the contact zone where gas (pores), electronic conductor and ionic conductor are present simultaneously and thus it is the only area where the electrochemical reaction can occur. If the electrode of an SOFC was made of a pure electronic conductor, the TPB would only be located at the interface between the electrode and electrolyte. In contrast, in composite electrodes, the TPB is extended throughout the entire electrode, which causes a reduction of the activation losses. Finally, another benefit of composite anodes is the presence of electrolytic particles between the nickel ones, preventing the agglomeration of the metal particles, this being an undesired phenomenon that causes a decrease in TPB, deterioration of the electrode and a decrease in cell performance over time.

In spite of the advantages offered, composite electrodes need accurate design, with attention to the choice of electrode thickness, composition (in terms of volume fraction of electron conducting/ionic conducting particles) and particle dimensions. Modelling can help in understanding the effects of the various design parameters, and can inform electrode optimisation. In the literature, several models have been proposed [4–9]; these can be divided into three families: single-pore models, random resistor network models and random packing sphere models. Our study belongs to the third category, in which the electrode is considered as a random packing of bimodal spheres (i.e. all the particles are considered as spherical; the ionic conducting particles are all considered to have the same radius r_{io}, and electronic conducting particles are all considered to have the same radius r_{el}). With this basic assumption, the results of percolation theory can be applied to evaluate the TPB and the effective conductivities of the electronic and ionic conducting particle clusters spanning the electrode.

This study was developed in several steps, starting with an analytical model which did not include a simulation of the phenomenon of gas diffusion in the electrode pores [4]. Recently, mass transport has also been included in the model [3]; a detailed discussion on the differences between the previous (analytical) and the current version of the model is given in [5]. The present paper reports results obtained from the complete model, including the simulation of mass transport phenomena. The main effects of mass transport on the electrode performance are discussed, together with some highlights on electrode optimisation.

2 Model formulation

In this paper, only the main equations of the model are reported; a complete description can be found in [5]. The electrode is assumed to be an SOFC anode, made of a random mixture of spherical ionic and electronic conducting particles. The main phenomena occurring in an SOFC anode are charge transfer, mass transfer and the electrochemical reaction.

The model is composed of two parts: an electrochemical one (Eq. 1), including charge transport, charge balance and electrochemical kinetics, and a diffusion part (Eqs. 3, 4), taking into account mass balances and mass transport equations.

In the electrochemical part of the model, Ohm's law has been applied for the charge transport, for both the ionic and electronic species. The resistivities used in Ohm's law are effective values (ρ^{eff}) obtained from the percolation theory [4]. Concerning the electrochemical reaction, the charge conservation is expressed by the charge balance equation, while the Butler–Volmer equation is used for the electrochemical kinetics. In the Butler–Volmer equation, the active area for the electrochemical reaction appears (A, active area per unit volume of the electrode), which is related to the TPB, and is calculated, again, by applying the equations of the percolation theory [4]. In Eq. 1, i_n is the transfer current density per unit of active area, while i_{io} and i_{el} are the ionic and electronic current densities, referred to as the cell area. More in detail, i_{io} and i_{el} are the current densities flowing along the x direction along the ionic and the electronic conductor, respectively, and their sum is equal to the overall current density I.

$$\begin{cases} \dfrac{\mathrm{d}V_{\text{io}}}{\mathrm{d}x} = -\rho_{\text{io}}^{\text{eff}} i_{\text{io}} \\ \dfrac{\mathrm{d}V_{\text{el}}}{\mathrm{d}x} = -\rho_{\text{el}}^{\text{eff}} i_{\text{el}} \\ \dfrac{\mathrm{d}i_{\text{io}}}{\mathrm{d}x} = -\dfrac{\mathrm{d}i_{\text{el}}}{\mathrm{d}x} \\ \dfrac{\mathrm{d}i_{\text{el}}}{\mathrm{d}x} = -A \cdot i_0 \left\{ \dfrac{p_{\text{H}_2}}{p_{\text{H}_2}^0} \exp\left(\dfrac{\beta\eta F}{RT}\right) \right. \\ \qquad \left. - \dfrac{p_{\text{H}_2\text{O}}}{p_{\text{H}_2\text{O}}^0} \exp\left(-(1-\beta)\dfrac{\eta F}{RT}\right) \right\} = -A \cdot i_n \\ \eta = \left(V_{\text{el}}^{\text{eq}} - V_{\text{io}}^{\text{eq}}\right) - \left(V_{\text{el}} - V_{\text{io}}\right) \end{cases} \tag{1}$$

For the second part of the model, the semi-reaction occurring at the anodic side of an SOFC is:

$$\text{H}_2 + \text{O}^{2-} \rightarrow \text{H}_2\text{O} + 2\text{e}^- \tag{2}$$

In an SOFC anode, the conversion of the oxygen ions and the formation of electrons is related to the consumption of H_2 and the formation of H_2O through Faraday's law; in light of this, the mass balances can be written as follows:

$$\begin{aligned} \frac{\mathrm{d}N_{\text{H}_2}}{\mathrm{d}x} &= -\frac{i_n}{2F}A \\ \frac{\mathrm{d}N_{\text{H}_2\text{O}}}{\mathrm{d}x} &= \frac{i_n}{2F}A \end{aligned} \tag{3}$$

where the molar fluxes are denoted with N and F is Faraday's constant. Using the theory for the diffusion in porous media [5, 10, 11], it is possible to derive expressions for the molar fluxes as:

$$\begin{aligned} N_{\text{H}_2} &= -\left(x_{\text{H}_2\text{O}} \left(\frac{1}{D_{\text{H}_2-\text{H}_2\text{O}}^{\text{eff}}} + \frac{1}{D_{\text{H}_2,K}^{\text{eff}}} \right)^{-1} \cdot \right. \\ &\quad \left. + x_{\text{H}_2} \left(\frac{1}{D_{\text{H}_2-\text{H}_2\text{O}}^{\text{eff}}} + \frac{1}{D_{\text{H}_2\text{O},K}^{\text{eff}}} \right)^{-1} \right) \cdot \frac{1}{RT} \frac{\mathrm{d}p_{\text{H}_2}}{\mathrm{d}x} \\ N_{\text{H}_2\text{O}} &= -\left(x_{\text{H}_2\text{O}} \left(\frac{1}{D_{\text{H}_2-\text{H}_2\text{O}}^{\text{eff}}} + \frac{1}{D_{\text{H}_2,K}^{\text{eff}}} \right)^{-1} \right. \\ &\quad \left. + x_{\text{H}_2} \left(\frac{1}{D_{\text{H}_2-\text{H}_2\text{O}}^{\text{eff}}} + \frac{1}{D_{\text{H}_2\text{O},K}^{\text{eff}}} \right)^{-1} \right) \cdot \frac{1}{RT} \frac{\mathrm{d}p_{\text{H}_2\text{O}}}{\mathrm{d}x} \end{aligned} \tag{4}$$

where the diffusivities are expressed according to the equations below [10]:

$$D_{i,K}^{\text{eff}} = \frac{\varepsilon}{\tau} .97 . r_{\text{pore}} \sqrt{\frac{T}{M_i}} \tag{5}$$

$$D_{\text{H}_2-\text{H}_2\text{O}}^{\text{eff}} = \frac{\varepsilon}{\tau} \cdot 0.0018583 \left(\frac{1}{M_{\text{H}_2}} + \frac{1}{M_{\text{H}_2\text{O}}} \right)^{1/2} \frac{T^{3/2}}{p \cdot \sigma^2 \cdot \Omega} \tag{6}$$

The Knudsen diffusivities D_K^{eff} play a role when diffusion occurs in a porous medium with pore radii smaller than the mean free path of the diffusing molecules. In solids formed by a random packing of bimodal spheres, the average pore radius is related to the radius of the electrode particles through the following equation [11, 12]:

$$r_{\text{pore}} = \frac{1}{1-\varepsilon} \left(\frac{\phi_{\text{el}}}{r_{\text{el}}} + \frac{1-\phi_{\text{el}}}{r_{\text{io}}} \right)^{-1} \tag{7}$$

where ϕ_{el} is the volumetric fraction of the electronic conductor and r_{el} and r_{io} are the radii of the electronic and ionic conducting particles, respectively.

In Fig. 2, the Knudsen diffusivities are reported for H_2 (Fig. 2a) and H_2O (Fig. 2b), together with the molecular diffusivities of the H_2/H_2O pair, as a function of the particle dimensions, at the typical operating temperature of SOFCs, about 1,173 K. The value of P is 1, which means that the radii of the electronic and ionic conducting particles composing the electrode are equal. Figure 2 shows that the Knudsen diffusivities are the dominating factor in the evaluation of the overall diffusivity for particles smaller than 0.7 μm for H_2O and 0.25 μm for H_2, respectively. However, the contribution of Knudsen diffusivities is still significant for particles up to 2 μm for H_2O and 1 μm for H_2, respectively.

In both parts of the model, several parameters are temperature and/or pressure dependent, and are conveyed through literature expressions. The equations used for the diffusivities are reported above (Eqs. 5, 6); the exchange current density i_0 is expressed according to the following equation [13]:

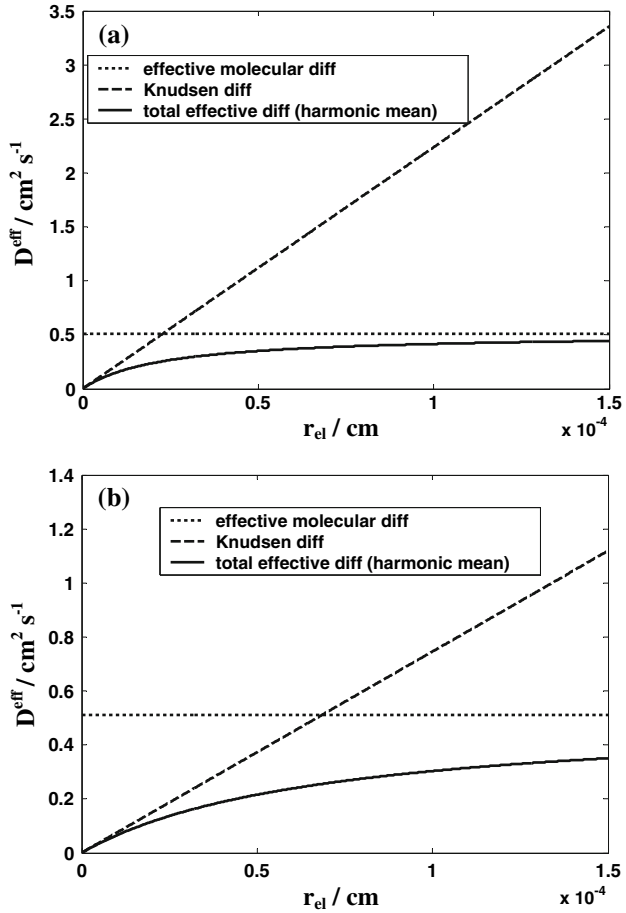

Fig. 2 Diffusivities of water (**a**) and hydrogen (**b**) as a function of the radius of the electronic conducting particle in the electrode ($P = 1$, $T = 1{,}173$ K, $p = 1$ atm)

$$i_0 = \gamma \left(\frac{p_{H_2}}{p_{ref}}\right) \left(\frac{p_{H_2O}}{p_{ref}}\right)^{-0.5} \exp\left(-\frac{E_{act}}{RT}\right) \quad (8)$$

Finally, the ionic resistivity of the electrolyte has also been assumed to be temperature dependent [14] (while the electronic conductivity of Ni has been approximated as constant):

$$\rho_{io} = \rho_{io}^0 \exp\left(\frac{E'_{act}}{RT}\right) \quad (9)$$

The two parts of the model, Eq. 1 and Eqs. 3, 4 cannot be solved separately, because the reaction takes place throughout the electrode and not only at the electrode–electrolyte interface; this is a distinctive feature of composite electrodes, and it links the electrical current and the mass fluxes to each other at each point in the electrode.

From a mathematical point of view, this is a boundary value problem and it has been solved numerically with Matlab [4]. Upon mathematical solution of the system of equations, the performance of the electrode is evaluated through its total overpotential (η), which is the difference between the theoretical reversible electrode voltage and the real operating voltage. This quantity takes into account three types of losses: activation, ohmic and concentration.

3 Results and discussion

Table 1 reports the values of the model parameters. In Fig. 3, η is shown as a function of the particle radius, for several electrode thicknesses. Figure 3 shows that the

Table 1 Model parameters (at $T = 1{,}173$ K, $p = 1$ atm)

Parameter	Value	Description
φ	0.4 (percolation thresholds: 0.294–0.706 with $P = 1$)	Volume fraction of electronic conducting particles [4]
σ_{el}	2×10^6 S m^{-1} (@900 °C)	Electronic conductivity of pure nickel [4]
σ_{io}	10 S m^{-1} (@900 °C)	Ionic conductivity of pure YSZ [14]
γ	2.9×10^4 A cm^{-2}	Pre-exponential factor in Eq. 8 (value from [13])
P	1	r_{io}/r_{el}
r_{el}	0.05–0.2 μm	Radius of electronic conducting particle
i_0	0.1 A cm^{-2} (@900 °C)	Exchange current density
β	0.5	Charge transfer coefficient
$p^0_{H_2}$	0.6–0.7 atm	H_2 partial pressure (inlet)
p_{ref}	1 atm	Reference pressure in Eq. 8
I	0.5 A cm^{-2}	Overall electrode current density
t	50–200 μm	Electrode thickness
ε	0.4	Electrode porosity
τ	7	Electrode tortuosity

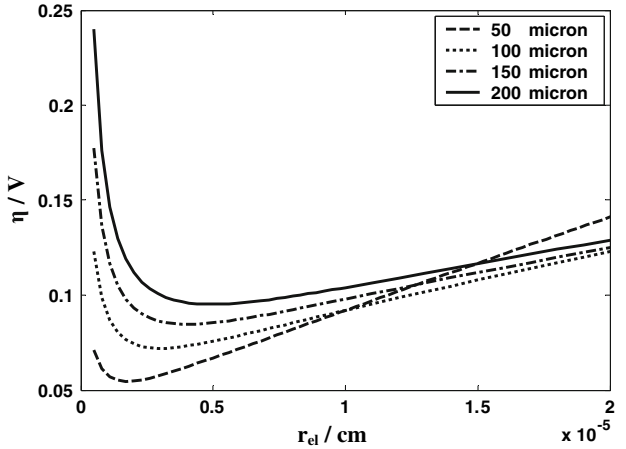

Fig. 3 Total electrode overpotential as a function of the radius of the electronic conducting particle in the electrode. Model parameters: $T = 1{,}173$ K, $p = 1$ atm, $p^0_{H_2} = 0.6$ atm. Varying parameter: overall electrode thickness (t)

curves representing η have a minimum, which is the trade-off between activation and concentration losses. Indeed, activation losses are reduced by an increase in the active area, which is achieved with small particles, which ensure a high area/volume ratio. In contrast, concentration losses are reduced when large pores are present, i.e. in electrodes formed by large particles. Thus, in Fig. 3, on the left-hand side (small particles), activation losses are small and concentration losses are large, while on the right-hand side the opposite happens.

In Fig. 4, η is reported as a function of the electrode thickness. Figure 4 shows that, for thicknesses up to about 50 μm, an increase in thickness causes a decrease in η, while above 50 μm, η increases with increasing electrode thickness. To explain this behaviour, we must consider that, for thin electrodes (<50 μm), the overall TPB in the

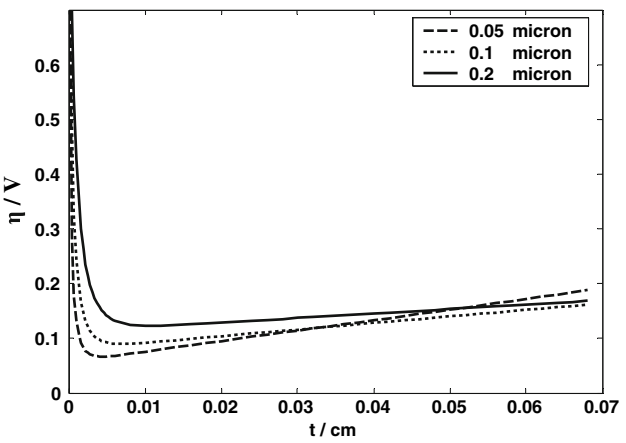

Fig. 4 Total electrode overpotential as a function of overall electrode thickness. Model parameters: $T = 1{,}173$ K, $p = 1$ atm, $p^0_{H_2} = 0.6$ atm. Varying parameter: radius of the electronic conducting particle in the electrode (r_{el})

electrode is limited, and thus an increase in electrode thickness leads to a significant increase in overall TPB. In practice, in this range, activation losses dominate. To analyse the electrode behaviour for thicknesses above 50 μm, two additional figures are presented (Figs. 5, 6). In Fig. 5, the overpotential along the thickness of the electrode is reported for three different particle dimensions and

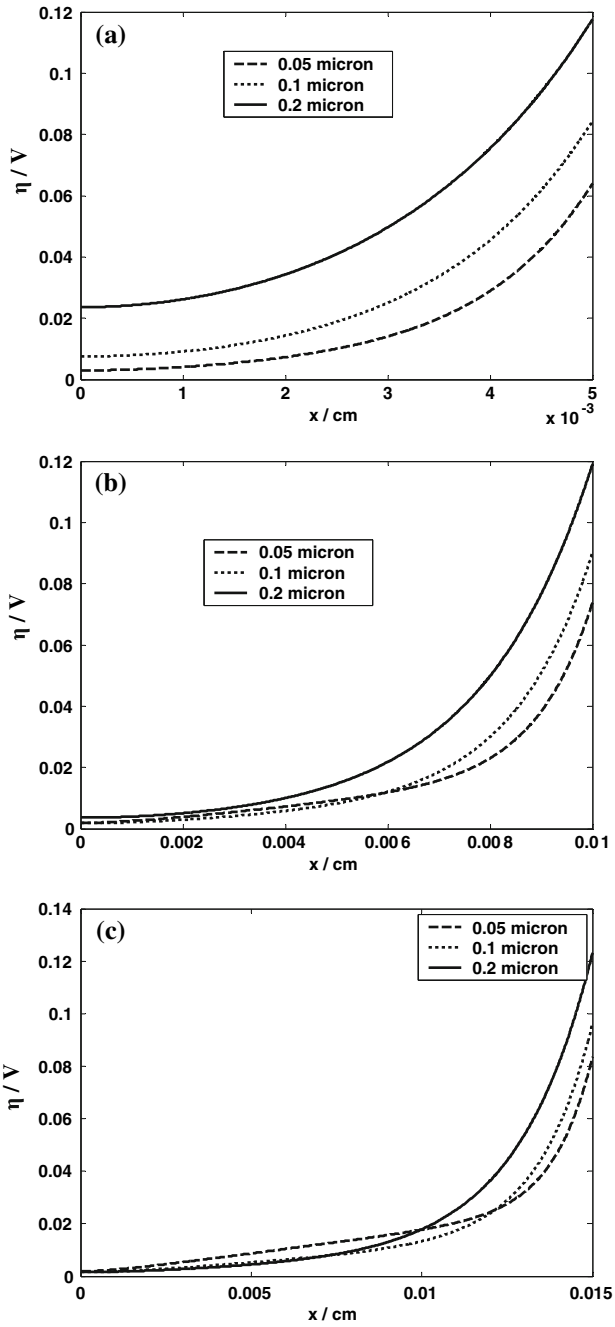

Fig. 5 Distribution of electrode overpotential along the x co-ordinate. Model parameters: $T = 1{,}173$ K, $p = 1$ atm, $x^0_{H_2} = 0.6$, overall electrode thickness: (**a**) 50 μm, (**b**) 100 μm, (**c**) 150 μm. Varying parameter: radius of the electronic conducting particle in the electrode (r_{el})

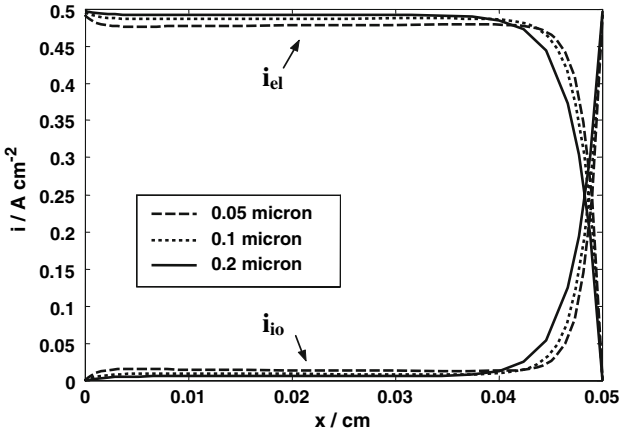

Fig. 6 Electronic and ionic current densities along the along the x co-ordinate. Model parameters: $T = 1{,}173$ K, $p = 1$ atm, $x^0_{H_2} = 0.6$. Varying parameter: radius of the electronic conducting particle in the electrode (r_{el})

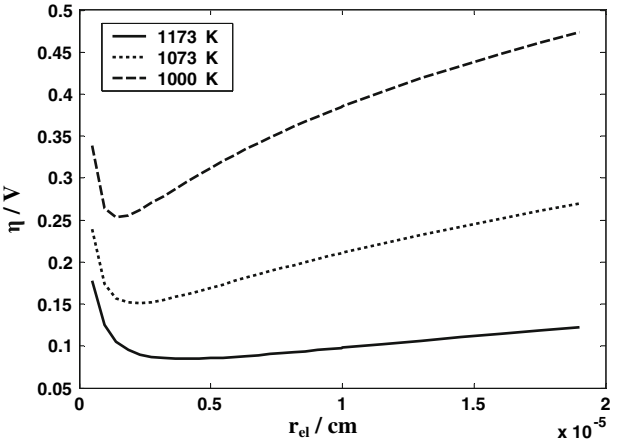

Fig. 7 Total electrode overpotential as a function of the radius of the electronic conducting particle in the electrode. Model parameters: $p^0_{H_2} = 0.6$ atm, thickness = 150 μm. Varying parameter: operating temperature (T)

for three thicknesses of the electrode [(a) 50 μm, (b) 100 μm and (c) 150 μm]. Considering that the rate of the local electrochemical reaction is related to the value of η (and that no electrochemical reaction occurs when the local value of η is 0), most of the electrochemical reaction takes place in the first 50 μm near the electrode/electrolyte interface for all the three electrode thicknesses and also for the three particle sizes. In the remaining part of the electrode, the only phenomenon taking place is that of charge conduction, which is electron conduction occurring along the electronic conducting phase within the electrodes. This is further demonstrated by Fig. 6, which shows that, for an electrode of thickness 500 μm, the current remains electronic up to a thickness of about 450 μm, and then becomes ionic in the 50 μm near the electrode/electrolyte interface, thanks to the electrochemical reaction which also occurs in this case in the 50 μm near the electrode/electrolyte interface.

In the light of this, by increasing the electrode thickness, the contribution of the ohmic losses is the same (due to the high electronic conductivity) for all the thicknesses. Thus, an increase in electrode thickness does not lead to an increase in ohmic loss. This is also confirmed by additional simulation results not reported here [5, 15]. Therefore, we can conclude that the increase of η as a function of the electrode thickness reported in Fig. 4 for electrode thicknesses between 50 and 700 μm is entirely due to concentration overpotential. As expected, the increase is steeper for electrodes with a small particle ratio, where diffusivities and, in particular, Knudsen diffusivities are lower. Obviously, these results hold for composite electrodes with high conductivity of the electronic conducting phase, such as the electrode under consideration, where the electronic conductor is a metal and the volume fraction composition is far away from the percolation threshold of the electronic conductor, the volume fraction of the electronic conductor is $\varphi = 0.4$, while the percolation threshold of the electronic conductor is $\varphi = 0.294$ (see Table 1). Also, these results are valid up to a certain electrode thickness (in the order of several mm for the electrode under consideration), above which ohmic losses along the electronic conductor of the electrode become significant. Usually, the electrode thicknesses above which these losses become significant are out of the application range of SOFC electrodes. A complete treatment can be found in a previous paper [15].

Figure 7 reports the effect of temperature on the electrode performance. An increase in the operating temperature causes (i) an exponential increase of the exchange current density (Eq. 6); (ii) an increase in diffusivity (proportional to $T^{1/2}$ for the Knudsen diffusivity, and to $T^{3/2}$ for the molecular diffusivity, Eqs. 7, 8); and (iii) an exponential decrease in ionic resistivity (Eq. 9). These phenomena lead to a global increase in electrode performance, which is represented in Fig. 7. Since the effect of temperature is more marked on activation losses than on concentration ones, the region where the activation losses are small compared to concentration (left-hand side of the graphs) becomes wider when the temperature is increased.

In Fig. 8, the trend of overpotential along the thickness of the electrode (x co-ordinate in Fig. 1) is reported, for three different operating temperatures. It is interesting to note that, generally speaking, the electrochemical reaction occurs mainly in a layer close to the electrode/electrolyte interface ($x = 150$ μm). This is shown by the fact that most overvoltages are concentrated in that area. With increasing temperature, overpotentials decrease and the layer where the electrochemical reaction takes place is also reduced, as

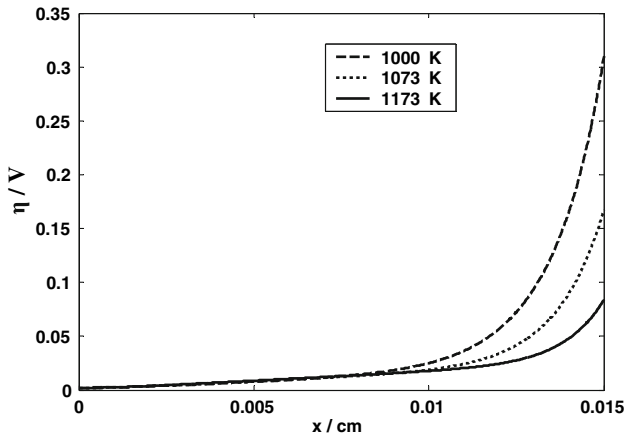

Fig. 8 Electrode overpotential along the x co-ordinate. Model parameters: $p = 1$ atm, $x^0_{H_2} = 0.6$, thickness = 150 μm, $r_{el} =$ 0.05 μm. Varying parameter: operating temperature (T)

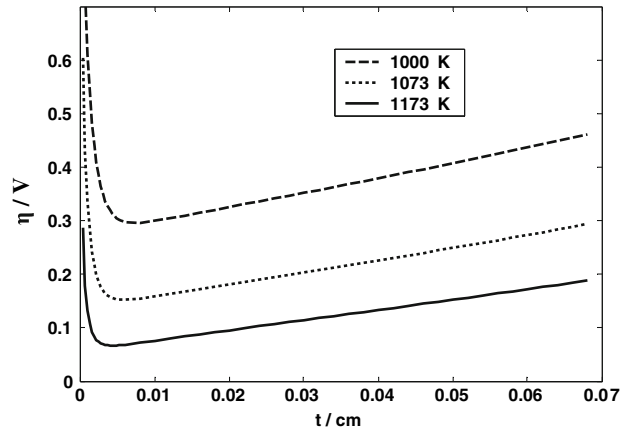

Fig. 9 Total electrode overpotential as a function of overall electrode thickness. Model parameters: $p^0_{H_2} = 0.6$ atm, particle radii = 0.05 μm. Varying parameter: operating temperature (T)

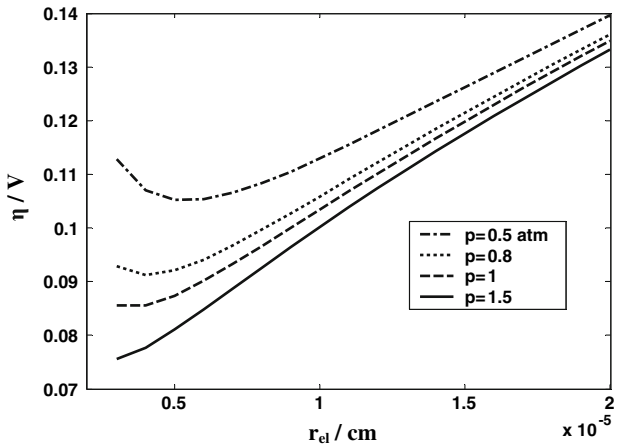

Fig. 10 Total electrode overpotential as a function of the radius of the electronic conducting particle in the electrode. Model parameters: $T = 1{,}173$ K, $x^0_{H_2} = 0.6$, thickness = 150 μm. Varying parameter: pressure (p)

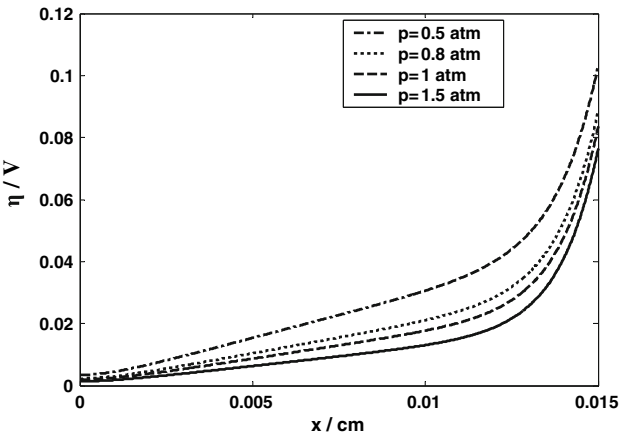

Fig. 11 Electrode overpotential along the x co-ordinate. Model parameters: $T = 1{,}173$ K, $x^0_{H_2} = 0.6$, thickness = 150 μm, $r_{el} =$ 0.05 μm. Varying parameter: pressure (p)

displayed in Fig. 8. For this reason, by increasing the operating temperature, the optimal value of the thickness is shifted to thinner electrodes, as shown in Fig. 9.

An increase in pressure reduces concentration losses (Eq. 4 coupled to Eqs. 5, 6); activation losses are also slightly reduced (Eq. 8), while ohmic losses are not influenced (Eq. 9). The increase in performance obtained by increasing the operating pressure is displayed in Fig. 10, which shows that the pressure effect is mainly evident for small particles (left-hand side of the plot), where concentration losses are dominant. For an operating pressure of 1.5 atm, the overall electrode loss, η, is as small as 0.075 V with electrode particles having a radius of 0.3 μm, with an electrode thickness of 150 μm. For large particles, where the main loss is due to activation, the lines representing the different operating pressures are quite close to each other and the graphs tend to superimpose.

Again, Fig. 11 shows the distribution of the overpotential along the electrode x co-ordinate. In this case, with increasing pressure the thickness of the electrode layer where the electrochemical reaction takes place remains approximately unchanged. As a consequence, as shown in Fig. 12, which displays the overall electrode loss as a function of the electrode thickness, the optimal value of the thickness remains approximately unchanged with varying pressure.

4 Conclusions

A complete model for composite electrodes has been presented, including an evaluation of concentration losses. In particular, the effect of mass transport on electrode performance has been analysed for various operating

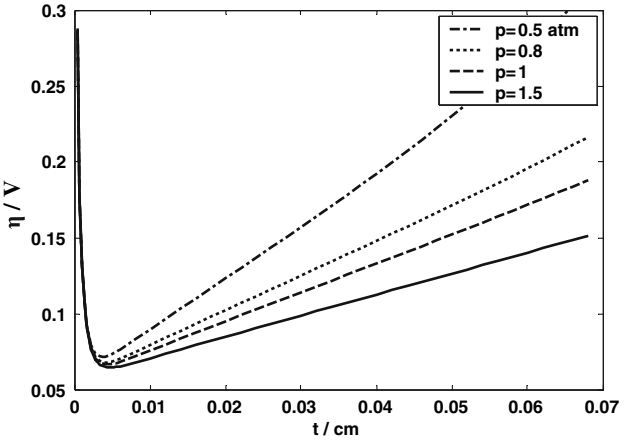

Fig. 12 Total electrode overpotential as a function of overall electrode thickness. Model parameters: $T = 1{,}173$ K, $x^0_{H_2} = 0.6$, particle radii = 0.05 μm. Varying parameter: pressure (p)

conditions. The model can be used as an optimisation tool in the design of SOFC anodes: indeed, the electrode performance is a function of its composition, thickness and microstructure and the electrode optimisation is a trade-off between the minimisation of activation and concentration losses. If possible, the operating conditions should also be taken into account in the optimisation phase, since they significantly influence the electrode performance.

Acknowledgements The authors thank Rolls-Royce Fuel Cell Systems Ltd and the European Union (European Contracts NNE5-2001-791 PIP-SOFC and SES6-CT-2003-502612 REAL-SOFC) for financial support during this work. Also, the authors acknowledge the British Council/CRUI project for funding an exchange of visits between Rolls-Royce Fuel Cell Systems Ltd and the University of Genoa.

References

1. Fuel Cell Handbook (2000) E.G. and G. Services Parsons Inc
2. Singhal C, Kendall K (2003) High temperature solid oxide fuel cells, fundamentals, design and applications. Elsevier, Amsterdam
3. Cannarozzo M (2005) Degree thesis. Effects of mass transport on the performance of composite electrodes for SOFC applications. DICHEP, University of Genoa, Genoa
4. Costamagna P, Costa P, Antonucci V (1998) Electrochim Acta 43(3–4):375–394
5. Cannarozzo M, Grosso S, Agnew G, Del Borghi A, Costamagna P (2007) J Fuel Cell Sci Technol 4(1):99–106
6. Costamagna P, Costa P, Arato E (1998) Electrochim Acta 43(8):967–972
7. Kenjo T, Osawa S, Fujikawa K (1991) J Electrochem Soc 138(2):349–355
8. Sunde S (1996) J Electrochem Soc 143(3):1123–1132
9. Abel J, Kornyshev AA, Lehnert W (1997) J Electrochem Soc 144(12):4253–4259
10. Bird RB, Stewart WE, Lightfoot EN (1960) Transport phenomena. Wiley, New York
11. Mason EA, Malinauskas AP (1983) Gas transport in porous media: the dusty-gas model. Elsevier
12. Krishna R, Wesselingh JA (2000) Mass transfer in multicomponent mixture. Delft University Press
13. Costamagna P, Honegger K (1991) J Electrochem Soc 138(2):349–355
14. Bossel UG (1992) Facts and figures. Final report on SOFC data, IEA report. Operating Task II, Swiss Federal Office of Energy, Berne
15. Costamagna P, Costa P, Arato E (1998) Electrochim Acta 43(8):967–972